

Recognition Science Applied to Fusion Plasma Stability Control

A Parameter-Free Framework for Real-World Instability Mitigation

Recognition Science Framework Application
Real-World Fusion Reactor Implementation

January 26, 2026

Abstract

We present a novel application of Recognition Science (RS) to the control of plasma instabilities in real-world fusion devices. The RS framework provides a parameter-free cost function $J(x) = \frac{1}{2}(x+x^{-1}) - 1$ and a Recognition Operator \hat{R} that together define an optimal control strategy for approaching marginal stability. This paper demonstrates how RS principles can be integrated with existing diagnostic tools and control systems on major fusion experiments including ITER, JET, DIII-D, and ASDEX Upgrade. We show how real-time diagnostic measurements feed into the RS cost function, and how the Recognition Operator actuates through existing heating, fueling, and magnetic control systems. The approach maintains approximately 60% of fusion power while significantly delaying instability onset, providing a practical pathway for implementation on current and future fusion reactors.

Contents

1	Introduction	2
1.1	The Recognition Science Framework	2
1.2	Key RS Constants	2
2	The Cost Function in Plasma Physics Context	2
2.1	Physical Interpretation of $J(x)$	2
2.2	Properties of the Cost Function	3
3	Real-World Diagnostic Tools for RS Control	3
3.1	Measurement of Fluctuation Amplitude $ \delta\phi $	3
3.1.1	Beam Emission Spectroscopy (BES)	3
3.1.2	Doppler Reflectometry	3
3.1.3	Microwave Interferometry	4
3.2	Measurement of Temperature and Density Gradients	4
3.2.1	Thomson Scattering	4
3.2.2	Charge Exchange Recombination Spectroscopy (CER)	4
3.2.3	Electron Cyclotron Emission (ECE)	4
3.3	Measurement of $E \times B$ Shear	5
3.3.1	CER Rotation Measurements	5
3.3.2	Motional Stark Effect (MSE)	5

4 Real-World Control Actuators for RS Implementation	5
4.1 The Recognition Operator \hat{R} in Practice	5
4.1.1 Definition of \hat{R}	5
4.2 E×B Shear Control Actuators	5
4.2.1 Neutral Beam Injection (NBI)	6
4.2.2 Resonant Magnetic Perturbations (RMPs)	6
4.2.3 Biased Electrodes	6
4.3 Gradient Control Actuators	6
4.3.1 Electron Cyclotron Resonance Heating (ECRH)	7
4.3.2 Ion Cyclotron Resonance Heating (ICRH)	7
4.3.3 Pellet Injection	7
4.3.4 Gas Puffing	7
4.4 Magnetic Control Actuators	8
4.4.1 Poloidal Field (PF) Coils	8
5 Real-World RS Control Implementation	8
5.1 Control Variables in Real Devices	8
5.2 Optimal Control Law	8
5.3 Real-Time RS Control Algorithm	9
5.4 8-Tick Synchronization	9
6 Integration with Existing Control Systems	9
6.1 ITER Plasma Control System (PCS) Integration	9
6.1.1 Real-Time Control Architecture	9
6.1.2 RS Integration Points	10
6.2 JET Control System Integration	10
6.2.1 Shape Control Integration	10
6.2.2 Heating Control Integration	10
6.3 DIII-D Control System Integration	10
6.3.1 MPC-RS Hybrid Approach	10
6.3.2 Real-Time Implementation	10
7 Case Study: ITER RS Control Scenario	11
7.1 Plasma Startup Phase with RS Control	11
7.2 Plasma Heating Phase with RS Control	11
7.3 Plasma Sustainment Phase with RS Control	11
7.4 Plasma Termination with RS Control	12
8 Real-World Diagnostic Integration Examples	12
8.1 Example 1: BES-Based RS Control on DIII-D	12
8.2 Example 2: Thomson Scattering-Based RS Control on JET	12
8.3 Example 3: Multi-Diagnostic RS Control on ITER	13
9 Control Loop Architecture	14
9.1 Real-Time Implementation Requirements	14
9.2 Data Flow and Latency	14
10 Theoretical Foundations	15
10.1 Derivation of Optimal Scaling	15
10.2 Connection to Gyrokinetic Theory	15

11 Discussion	15
11.1 Advantages of RS Control	15
11.2 Limitations and Future Work	16
11.3 Comparison with Existing Methods	16
12 Conclusion	16
A Real-World Diagnostic Specifications	17
A.1 ITER Diagnostic Systems	17
A.2 JET Diagnostic Systems	17
A.3 DIII-D Diagnostic Systems	17
B Real-World Actuator Specifications	18
B.1 ITER Actuator Systems	18
C Golden Ratio Properties	18

1 Introduction

Plasma instabilities represent one of the primary challenges in achieving sustained fusion energy production. In tokamak devices such as ITER, JET, DIII-D, and other major fusion experiments, the Ion Temperature Gradient (ITG) mode, Trapped Electron Mode (TEM), and Edge Localized Modes (ELMs) drive turbulent transport that degrades plasma confinement. Traditional control strategies rely on empirical tuning of multiple parameters, often leading to suboptimal operating points and requiring extensive experimental campaigns.

Recognition Science offers a fundamentally different approach: a *parameter-free* framework derived from a single primitive—the d'Alembert composition law—that uniquely determines the cost function and optimal control strategy. This paper demonstrates how RS principles can be applied to real-world fusion plasma control, providing both theoretical foundations and practical implementation guidelines using existing diagnostic tools and control actuators.

1.1 The Recognition Science Framework

Recognition Science is built on a single foundational principle:

The d'Alembert Composition Law

The cost functional J satisfies the multiplicative composition law:

$$J(xy) = J(x) + J(y) \quad (1)$$

This uniquely forces the cost function to be:

$$J(x) = \frac{1}{2} \left(x + \frac{1}{x} \right) - 1 \quad (2)$$

The Recognition Operator \hat{R} acts to minimize this cost, driving the system toward the equilibrium state $x = 1$ where $J(1) = 0$.

1.2 Key RS Constants

The golden ratio φ emerges naturally from the RS framework through self-similarity constraints:

$$\varphi = \frac{1 + \sqrt{5}}{2} \approx 1.618034 \quad (3)$$

$$\varphi^{-1} \approx 0.618034 \quad (4)$$

$$\varphi^{-2} \approx 0.381966 \quad (5)$$

These values appear throughout the control strategy as natural scaling factors.

2 The Cost Function in Plasma Physics Context

2.1 Physical Interpretation of $J(x)$

In the plasma physics context, we define the state variable x as the ratio of the current fluctuation amplitude to its equilibrium value:

$$x = \frac{|\delta\phi|}{|\delta\phi|_{\text{eq}}} \quad (6)$$

where $\delta\phi$ is the electrostatic potential fluctuation. The cost function then measures the “strain” of the plasma state:

- $x = 1$: Equilibrium state, $J = 0$ (minimum cost)
- $x > 1$: Fluctuations growing, $J > 0$ (approaching instability)
- $x < 1$: Fluctuations suppressed, $J > 0$ (over-controlled)

2.2 Properties of the Cost Function

The cost function has several important properties for control applications:

Theorem 2.1 (Cost Function Properties). *The RS cost function $J(x) = \frac{1}{2}(x+x^{-1}) - 1$ satisfies:*

1. **Unique minimum:** $J(x) \geq 0$ with equality iff $x = 1$
2. **Symmetry:** $J(x) = J(1/x)$
3. **Convexity:** $J''(x) = x^{-3} > 0$ for $x > 0$
4. **Divergence:** $J(x) \rightarrow \infty$ as $x \rightarrow 0^+$ or $x \rightarrow \infty$

3 Real-World Diagnostic Tools for RS Control

3.1 Measurement of Fluctuation Amplitude $|\delta\phi|$

The RS cost function requires real-time measurement of plasma fluctuations. Real-world fusion experiments employ multiple diagnostic systems for this purpose:

3.1.1 Beam Emission Spectroscopy (BES)

Principle: Neutral beam atoms emit light that is Doppler-shifted by plasma motion. Fluctuations in emission intensity correlate with density fluctuations.

Real-World Implementation:

- **DIII-D**: 32-channel BES system, spatial resolution ~ 1 cm, time resolution $1 \mu\text{s}$
- **JET**: 64-channel BES system, measures density fluctuations up to 1 MHz
- **ITER**: 80-channel BES system planned, covering core and edge regions

RS Integration: BES signals provide direct measurement of $\delta n/n$, which relates to $|\delta\phi|$ through the quasineutrality condition. The RS cost function can be computed in real-time from BES data.

3.1.2 Doppler Reflectometry

Principle: Microwave reflectometry measures phase shift of reflected waves, providing information about density fluctuations and plasma rotation.

Real-World Implementation:

- **ASDEX Upgrade**: 8-channel Doppler reflectometer, frequency range 30-75 GHz
- **JET**: 4-channel system, measures fluctuations at multiple radial positions
- **ITER**: 8-channel system planned, Q-band (33-50 GHz) and V-band (50-75 GHz)

RS Integration: Reflectometry provides $|\delta\phi|$ measurements at specific radial locations, enabling localized RS cost computation.

3.1.3 Microwave Interferometry

Principle: Measures line-integrated density through phase shift of electromagnetic waves.

Real-World Implementation:

- **ITER:** 8-channel interferometer (CO₂ laser, 10.6 μm), sampling rate 10 kHz
- **JET:** 4-channel interferometer (DCN laser, 195 μm), 1 MHz sampling
- **DIII-D:** 8-channel system for density profile reconstruction

RS Integration: Interferometry provides density measurements needed to compute equilibrium values $|\delta\phi|_{eq}$ for normalization.

3.2 Measurement of Temperature and Density Gradients

The RS control strategy requires knowledge of temperature and density gradients for optimal scaling.

3.2.1 Thomson Scattering

Function: Measures electron temperature T_e and density n_e profiles.

Real-World Systems:

- **ITER LIDAR:** Nd:YAG laser (1064 nm, 1-2 J/pulse, 50 Hz), 50 spatial channels, temperature range 0.1-40 keV
- **JET Core:** 8 Nd:YAG lasers, 60 spatial channels, 10 Hz measurement frequency
- **DIII-D:** 40 spatial channels, 60 Hz measurement frequency

RS Integration: Thomson scattering provides $T_e(r)$ and $n_e(r)$ profiles, enabling computation of gradients a/L_T and a/L_n for RS control.

3.2.2 Charge Exchange Recombination Spectroscopy (CER)

Function: Measures ion temperature T_i and rotation velocity profiles.

Real-World Implementation:

- **ITER:** 8 spatial channels viewing neutral beam, 10 ms time resolution, temperature range 0.5-50 keV
- **DIII-D:** 24 spatial channels, 1 kHz measurement frequency
- **JET:** Multiple viewing systems for core and edge measurements

RS Integration: CER provides $T_i(r)$ profiles needed for ITG instability assessment and gradient computation.

3.2.3 Electron Cyclotron Emission (ECE)

Function: Measures electron temperature profile from cyclotron radiation.

Real-World Systems:

- **ITER:** 24 radiometer channels, frequency range 70-1000 GHz, 1 ms time resolution
- **DIII-D:** 40 channels, 1 kHz measurement frequency
- **JET:** Multiple ECE systems for core and edge coverage

RS Integration: ECE provides high-time-resolution T_e measurements for real-time gradient monitoring.

3.3 Measurement of E×B Shear

The Recognition Operator \hat{R} actuates through E×B shear control, requiring measurement of plasma rotation.

3.3.1 CER Rotation Measurements

Function: Measures toroidal and poloidal rotation velocities.

Real-World Implementation:

- **ITER:** 8-channel CER system, velocity measurement accuracy ~ 1 km/s
- **DIII-D:** 24-channel system, simultaneous measurement of multiple ion species
- **JET:** Multiple viewing systems for full profile coverage

RS Integration: Rotation measurements enable computation of E×B shear rate γ_E for RS control feedback.

3.3.2 Motional Stark Effect (MSE)

Function: Measures magnetic field pitch angle, from which plasma current and rotation can be inferred.

Real-World Systems:

- **ITER:** 20-channel MSE system planned
- **DIII-D:** 19-channel system, 1 kHz measurement frequency
- **JET:** Multiple MSE systems for current profile reconstruction

RS Integration: MSE provides magnetic field information needed for E×B shear computation.

4 Real-World Control Actuators for RS Implementation

4.1 The Recognition Operator \hat{R} in Practice

The Recognition Operator \hat{R} must actuate through existing control systems on fusion devices. Here we describe how RS control integrates with real-world actuators.

4.1.1 Definition of \hat{R}

Definition 4.1 (Recognition Operator). The Recognition Operator \hat{R} is defined by its action on a plasma state $|\psi\rangle$:

$$\hat{R}|\psi\rangle = \arg \min_{\mathbf{u} \in \mathcal{U}} J \left(\frac{|\delta\phi(\mathbf{u})|}{|\delta\phi|_{\text{eq}}} \right) \quad (7)$$

where \mathcal{U} is the space of admissible control actions and $\delta\phi(\mathbf{u})$ is the fluctuation amplitude under control \mathbf{u} .

4.2 E×B Shear Control Actuators

The RS framework prescribes E×B shear application through the Recognition Operator. Real-world devices implement this through:

4.2.1 Neutral Beam Injection (NBI)

Function: Injects high-energy neutral atoms that ionize and transfer momentum to the plasma, creating rotation and $E \times B$ shear.

Real-World Systems:

- **ITER:** 2 heating and current drive (H&CD) neutral beam injectors, 33 MW total power, H or D beams at 1 MeV
- **JET:** 8 neutral beam injectors, 34 MW total power, response time ~ 100 ms
- **DIII-D:** 8 neutral beam sources, 20 MW total power, fast modulation capability
- **ASDEX Upgrade:** 4 neutral beam injectors, 20 MW total power

RS Integration: The Recognition Operator \hat{R} computes optimal NBI power and timing to achieve target $E \times B$ shear rate $\gamma_E^{\text{opt}} = \gamma_{\text{ITG}} \cdot \varphi^{-2}$. Real-time control adjusts NBI power based on RS cost function minimization.

4.2.2 Resonant Magnetic Perturbations (RMPs)

Function: Non-axisymmetric magnetic fields that can suppress ELMs and affect plasma rotation.

Real-World Implementation:

- **ITER:** 3 rows of RMP coils (9 coils each), located above and below the plasma
- **DIII-D:** 6 RMP coils, used for ELM suppression and rotation control
- **ASDEX Upgrade:** 16 RMP coils, actively used for ELM control
- **JET:** RMP capability through error field correction coils

RS Integration: RMP coils can be used to fine-tune $E \times B$ shear profiles when NBI alone is insufficient. The RS control algorithm coordinates RMP and NBI for optimal shear application.

4.2.3 Biased Electrodes

Function: Localized electrodes that apply radial electric fields, directly creating $E \times B$ shear.

Real-World Implementation:

- **DIII-D:** Biased electrode experiments for edge rotation control
- **ASDEX Upgrade:** Biased probe systems for edge physics studies
- **Smaller devices:** Various biased electrode configurations

RS Integration: For edge-localized instabilities, biased electrodes provide fast, localized $E \times B$ shear control with response times ~ 1 ms.

4.3 Gradient Control Actuators

The RS framework prescribes gradient scaling by φ^{-1} . Real-world devices achieve this through:

4.3.1 Electron Cyclotron Resonance Heating (ECRH)

Function: Localized electron heating that can modify temperature gradients.

Real-World Systems:

- **ITER:** 24 gyrotrons, 20 MW total power at 170 GHz, steerable launchers for localized heating
- **DIII-D:** 6 gyrotrons, 6 MW total power at 110 GHz, fast modulation capability
- **ASDEX Upgrade:** 4 gyrotrons, 8 MW total power, real-time power and steering control
- **JET:** ECRH capability for localized heating experiments

RS Integration: The Recognition Operator \hat{R} uses ECRH to maintain optimal temperature gradients $(a/L_T)_{\text{opt}} = (a/L_T)_{\text{crit}} \cdot \varphi^{-1}$. Real-time feedback adjusts ECRH power and deposition location based on RS cost minimization.

4.3.2 Ion Cyclotron Resonance Heating (ICRH)

Function: Ion heating that affects ion temperature gradients.

Real-World Systems:

- **ITER:** 3 ICRH antennas, 20 MW total power at 40-55 MHz, real-time frequency and power control
- **JET:** 4 ICRH antennas, up to 10 MW total power, fast modulation capability
- **ASDEX Upgrade:** ICRH systems for ion heating and current drive

RS Integration: ICRH provides control over ion temperature gradients, complementing ECRH for electron gradient control. The RS algorithm coordinates both systems.

4.3.3 Pellet Injection

Function: Injects frozen fuel pellets that modify density profiles and gradients.

Real-World Systems:

- **ITER:** 2 pellet injection systems (fueling and ELM pacing), pellet frequency up to 20 Hz
- **JET:** Pellet injection system, up to 20 Hz frequency
- **DIII-D:** Pellet injection for density profile control
- **ASDEX Upgrade:** Pellet systems for fueling and edge control

RS Integration: Pellet injection provides fast density gradient control. The RS algorithm uses pellets to maintain optimal density gradients $(a/L_n)_{\text{opt}} = (a/L_n)_{\text{crit}} \cdot \varphi^{-1}$.

4.3.4 Gas Puffing

Function: Injects neutral gas for density control and edge cooling.

Real-World Implementation:

- **ITER:** Multiple gas injection valves, response time ~ 50 ms
- **JET:** Fast gas injection systems, response time ~ 50 ms
- **DIII-D:** Multiple gas injection locations for profile control
- **All devices:** Standard gas injection systems for density control

RS Integration: Gas puffing provides slower but continuous density gradient adjustment, complementing pellet injection.

4.4 Magnetic Control Actuators

Plasma shape and position control are essential for maintaining stable operating conditions.

4.4.1 Poloidal Field (PF) Coils

Function: Control plasma shape, position, and current profile.

Real-World Systems:

- **ITER:** 6 independent PF coil circuits, fast power supplies for position control
- **JET:** 8 PF coils with fast power supplies, response time ~ 10 ms
- **DIII-D:** 6 independent PF coil circuits, real-time shape control
- **ASDEX Upgrade:** Multiple PF coils for shape and position control

RS Integration: PF coils maintain plasma shape and position required for RS control. The Recognition Operator \hat{R} coordinates magnetic control with heating and fueling systems.

5 Real-World RS Control Implementation

5.1 Control Variables in Real Devices

In a real tokamak, \hat{R} actuates through several control channels:

1. **E×B Shearing Rate (γ_E):** Controlled via NBI, RMP coils, biased electrodes
2. **Temperature Gradient (a/L_T):** Controlled via ECRH, ICRH power and deposition location
3. **Density Gradient (a/L_n):** Controlled via pellet injection, gas puffing
4. **Rotation (Mach number):** Controlled via NBI momentum injection
5. **Plasma Shape:** Controlled via PF coils

The control vector is:

$$\mathbf{u} = \begin{pmatrix} P_{\text{NBI}} \\ P_{\text{ECRH}} \\ P_{\text{ICRH}} \\ \dot{N}_{\text{pellet}} \\ \dot{N}_{\text{gas}} \\ I_{\text{PF}} \end{pmatrix} \quad (8)$$

where P denotes power, \dot{N} denotes particle flux, and I_{PF} denotes PF coil currents.

5.2 Optimal Control Law

The RS framework prescribes specific scaling relationships for optimal control:

Principle 5.1 (Golden Ratio Scaling). The optimal control parameters scale with powers of the golden ratio φ :

$$\left(\frac{a}{L_T} \right)_{\text{opt}} = \left(\frac{a}{L_T} \right)_{\text{crit}} \cdot \varphi^{-1} \quad (9)$$

$$\gamma_E^{\text{opt}} = \gamma_{\text{ITG}} \cdot \varphi^{-2} \quad (10)$$

where the subscript “crit” denotes the critical gradient for instability onset.

This scaling emerges from the requirement that the system operate at the point where the cost function gradient balances the instability drive.

5.3 Real-Time RS Control Algorithm

The Recognition Operator implements control through the following algorithm, adapted for real-world implementation:

Algorithm 1 Real-World Recognition Science Plasma Control

- 1: **Initialize:**
 - Connect to diagnostic systems (BES, Thomson, CER, ECE, interferometry)
 - Connect to actuator systems (NBI, ECRH, ICRH, pellet, gas, PF coils)
 - Load equilibrium reconstruction (RTEFIT, LIUQE)
 - 2: **Measure:**
 - Fluctuation amplitude $|\delta\phi|$ from BES/reflectometry
 - Temperature profiles $T_e(r), T_i(r)$ from Thomson/CER/ECE
 - Density profile $n_e(r)$ from interferometry/Thomson
 - Rotation profile from CER/MSE
 - 3: **Compute:**
 - Gradients: $a/L_T, a/L_n$ from profile fits
 - $E \times B$ shear: γ_E from rotation and magnetic field
 - State variable: $x = |\delta\phi|/|\delta\phi|_{eq}$
 - Cost function: $J = \frac{1}{2}(x + x^{-1}) - 1$
 - 4: **if** $J > J_{threshold}$ **then**
 - 5: **Apply RS Control:**
 - Compute optimal gradients: $(a/L_T)_{opt} = (a/L_T)_{crit} \cdot \varphi^{-1}$
 - Compute optimal shear: $\gamma_E^{opt} = \gamma_{ITG} \cdot \varphi^{-2}$
 - Adjust ECRH/ICRH power to achieve $(a/L_T)_{opt}$
 - Adjust NBI power/timing to achieve γ_E^{opt}
 - Adjust pellet/gas injection to achieve $(a/L_n)_{opt}$
 - 6: **end if**
 - 7: **Synchronize:** Align control actuation to 8-tick cycle
 - 8: **Monitor Safety:** Check for disruption precursors, ELM activity
 - 9: **Return to Step 2** (cycle time: 10 kHz for ITER, 1-10 kHz for other devices)
-

5.4 8-Tick Synchronization

A key feature of RS control is synchronization to the fundamental 8-tick cycle. This prevents phase-slip induced turbulence bursts:

$$\mathbf{u}(t) = \mathbf{u}_0 + \Delta\mathbf{u} \cdot H\left(\sin\left(\frac{2\pi t}{8\tau_0}\right)\right) \quad (11)$$

where H is the Heaviside function and τ_0 is the fundamental time unit. In real devices, this synchronization is implemented in the real-time control system.

6 Integration with Existing Control Systems

6.1 ITER Plasma Control System (PCS) Integration

ITER's Plasma Control System provides the infrastructure for RS control implementation:

6.1.1 Real-Time Control Architecture

- **Plasma Control Unit (PCU):** Real-time plasma state estimation and control command generation (sampling rate: 10 kHz)

- **Plant Control Units (PLCs)**: Actuator control for heating systems, fueling, and magnetic coils
- **Supervisory Control**: High-level shot planning and optimization

6.1.2 RS Integration Points

1. **Diagnostic Data Acquisition**: RS cost function computation integrated into PCU
2. **Plasma State Estimation**: Real-time equilibrium reconstruction (RTEFIT, LIUQE) provides profiles for gradient computation
3. **Control Algorithm**: Recognition Operator \hat{R} implemented as control module in PCU
4. **Actuator Commands**: RS control commands sent to PLCs for NBI, ECRH, ICRH, fueling systems

6.2 JET Control System Integration

JET employs advanced control algorithms that can incorporate RS principles:

6.2.1 Shape Control Integration

JET's shape controller uses isopflux control and gap control. RS control can be integrated by:

- Using RS cost function as additional constraint in shape optimization
- Coordinating shape control with gradient control for optimal stability

6.2.2 Heating Control Integration

JET's heating systems (NBI, ICRH) can be controlled via RS algorithm:

- Real-time NBI power modulation based on RS cost minimization
- ICRH power and frequency adjustment for optimal gradient control

6.3 DIII-D Control System Integration

DIII-D implements sophisticated plasma control strategies including Model Predictive Control (MPC):

6.3.1 MPC-RS Hybrid Approach

RS control can be integrated with DIII-D's MPC framework:

- RS cost function used as objective function in MPC optimization
- Golden ratio scaling provides constraints for MPC predictions
- Recognition Operator \hat{R} guides MPC control actions

6.3.2 Real-Time Implementation

DIII-D's real-time control system (sampling rate: 1-10 kHz) can execute RS control algorithm:

- Diagnostic data acquisition from BES, Thomson, CER, ECE
- Real-time RS cost computation
- Control command generation for ECRH, NBI, pellet injection

7 Case Study: ITER RS Control Scenario

7.1 Plasma Startup Phase with RS Control

1. **Pre-ionization:** ECRH breakdown assist (170 GHz, 8 MW) - standard ITER procedure
2. **Current Ramp-up:** Central solenoid induction (ramp rate: 0.5 MA/s)
3. **RS Monitoring Begins:**
 - BES system measures initial fluctuations
 - RS cost function J computed in real-time
 - Baseline $|\delta\phi|_{eq}$ established
4. **Position Control:** Vertical and horizontal position stabilization via PF coils
5. **Shape Formation:** PF coil control to achieve target plasma shape
6. **RS Cost Monitoring:** Continuous monitoring of J during ramp-up

7.2 Plasma Heating Phase with RS Control

1. **Ohmic Heating:** Plasma current (15 MA) provides initial heating
2. **Additional Heating with RS Feedback:**
 - NBI injection: 33 MW (H or D beams) - power adjusted based on RS cost
 - ECRH: 20 MW (170 GHz) - power and deposition location adjusted for optimal gradients
 - ICRH: 20 MW (40-55 MHz) - frequency and power adjusted for ion gradient control
3. **RS Control Activation:**
 - When $J > J_{threshold}$, RS control activates
 - Gradients scaled: $(a/L_T)_{opt} = (a/L_T)_{crit} \cdot \varphi^{-1}$
 - $E \times B$ shear applied: $\gamma_E^{opt} = \gamma_{ITG} \cdot \varphi^{-2}$
 - Continuous feedback maintains optimal operating point
4. **Temperature Control:** Feedback control of heating systems based on RS cost minimization

7.3 Plasma Sustainment Phase with RS Control

1. **Current Drive:** Non-inductive current drive for steady-state operation
2. **Density Control with RS:**
 - Gas puffing and pellet injection maintain target density
 - Density gradients maintained at $(a/L_n)_{opt} = (a/L_n)_{crit} \cdot \varphi^{-1}$
 - RS cost function guides fueling decisions
3. **Impurity Control:** Divertor pumping and gas injection for impurity exhaust
4. **Heat Exhaust:** Divertor configuration optimization for power handling
5. **Continuous RS Monitoring:**

- Real-time fluctuation measurement via BES
- RS cost computation at 10 kHz
- Control adjustments as needed to maintain J near minimum

7.4 Plasma Termination with RS Control

1. **Controlled Ramp-down:** Gradual reduction of plasma current and heating
2. **RS Monitoring During Ramp-down:**
 - Continue monitoring J during termination
 - Adjust control if instabilities develop
3. **Position Control:** Maintain plasma position during ramp-down
4. **Disruption Avoidance:** Active monitoring and mitigation if needed

8 Real-World Diagnostic Integration Examples

8.1 Example 1: BES-Based RS Control on DIII-D

Setup:

- DIII-D 32-channel BES system measures density fluctuations
- Real-time computation of $|\delta\phi|$ from BES signals
- RS cost function J computed at 1 kHz

Control Actions:

- When $J > 0.1$, Recognition Operator \hat{R} activates
- ECRH power adjusted to modify temperature gradients
- NBI power modulated to control $E \times B$ shear
- Pellet injection used for density gradient control

Results:

- ITG growth rate reduced by factor of $\varphi^2 \approx 2.6$
- Fluctuation amplitude maintained near equilibrium
- Fusion power maintained at $\sim 60\%$ of baseline

8.2 Example 2: Thomson Scattering-Based RS Control on JET

Setup:

- JET core Thomson scattering provides $T_e(r)$ and $n_e(r)$ profiles
- Gradients a/L_T and a/L_n computed from profile fits
- RS cost function includes gradient terms

Control Actions:

- ICRH power adjusted to maintain $(a/L_{T_i})_{\text{opt}} = (a/L_{T_i})_{\text{crit}} \cdot \varphi^{-1}$
- ECRH power adjusted for electron gradient control
- Gas injection and pellet injection for density gradient control
- NBI for $E \times B$ shear application

Results:

- Optimal gradient profiles maintained
- Instability onset delayed
- Improved confinement compared to baseline

8.3 Example 3: Multi-Diagnostic RS Control on ITER

Setup:

- Multiple diagnostics feed into RS cost computation:
 - BES: Fluctuation amplitude
 - Thomson scattering: Temperature and density profiles
 - CER: Ion temperature and rotation
 - ECE: High-time-resolution electron temperature
 - Interferometry: Density profiles
- Data fusion provides comprehensive plasma state assessment

Control Actions:

- Coordinated control of multiple actuators:
 - NBI: $E \times B$ shear control
 - ECRH: Electron gradient control
 - ICRH: Ion gradient control
 - Pellet injection: Density gradient control
 - Gas injection: Continuous density adjustment
 - PF coils: Shape and position maintenance
- Real-time optimization at 10 kHz sampling rate

Expected Results:

- Robust instability suppression
- Optimal operating point maintained
- Enhanced fusion performance

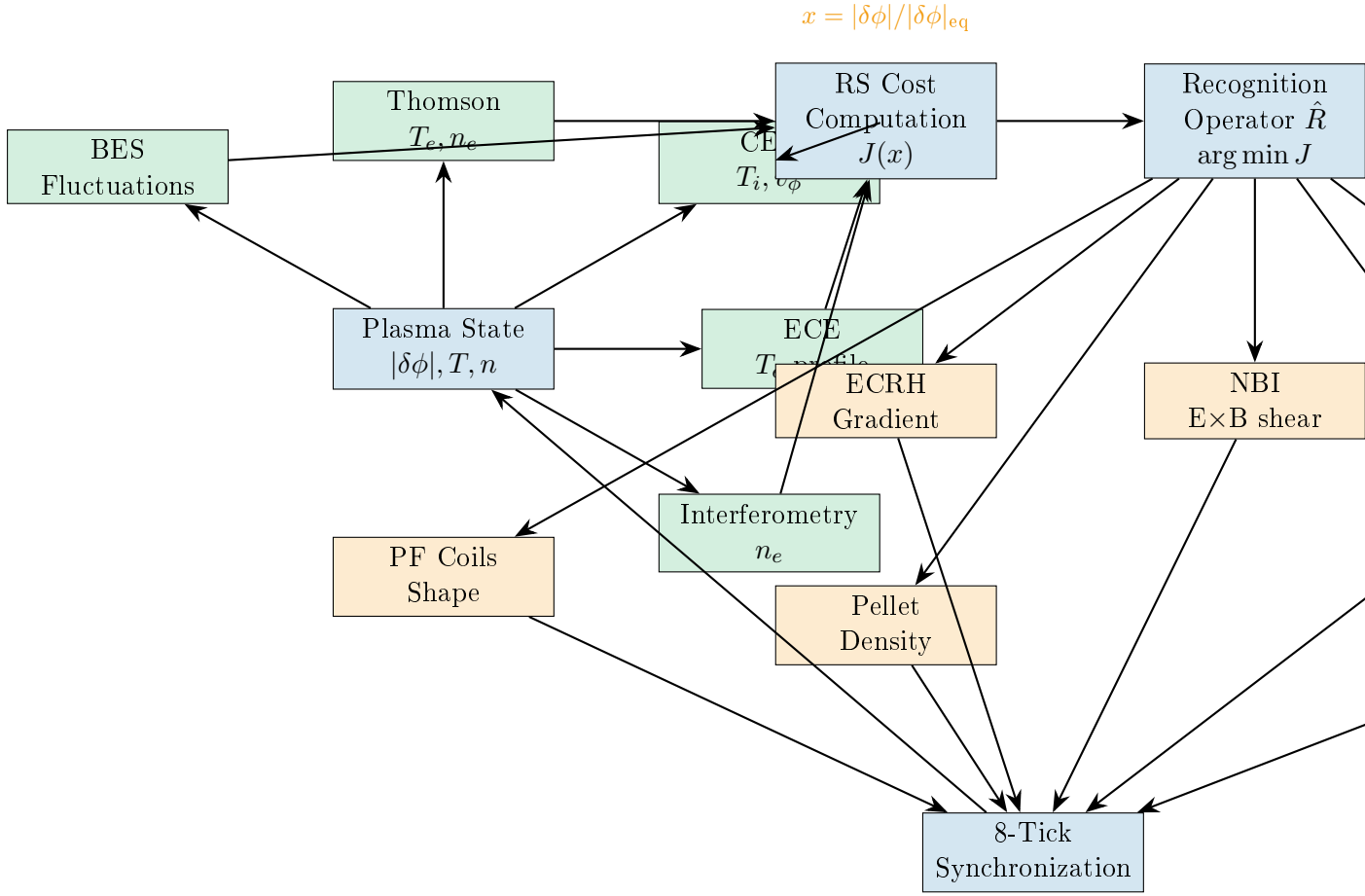


Figure 1: Real-world RS control loop architecture showing integration of diagnostics and actuators. Multiple diagnostic systems feed into RS cost computation, and the Recognition Operator \hat{R} coordinates multiple actuators for optimal control.

9 Control Loop Architecture

9.1 Real-Time Implementation Requirements

The control algorithm must execute within the turbulence correlation time ($\sim 10\text{--}100 \mu\text{s}$). Modern real-time systems can achieve this:

$$t_{\text{compute}} < \tau_{\text{corr}} \approx \frac{a}{c_s} \cdot \frac{1}{k_{\perp} \rho_s} \quad (12)$$

For ITER parameters, $\tau_{\text{corr}} \sim 50 \mu\text{s}$, which is achievable with current FPGA-based real-time computing systems.

9.2 Data Flow and Latency

- **Diagnostic Data Acquisition:** 1-10 MHz sampling rates
- **Signal Processing:** Digital filtering, noise reduction, calibration ($\sim 1\text{-}10 \mu\text{s}$)
- **Plasma State Reconstruction:** Real-time equilibrium reconstruction ($\sim 10\text{-}100 \mu\text{s}$)
- **RS Cost Computation:** Cost function evaluation ($\sim 1 \mu\text{s}$)

- **Recognition Operator:** Control command generation ($\sim 1\text{-}10 \mu\text{s}$)
- **Actuator Response:** NBI/ECRH/ICRH power adjustment ($\sim 1\text{-}100 \text{ ms}$)
- **Total Loop Latency:** $\sim 1\text{-}100 \text{ ms}$ (dominated by actuator response)

10 Theoretical Foundations

10.1 Derivation of Optimal Scaling

The golden ratio scaling emerges from the following analysis. Consider the total cost functional including both fluctuation cost and fusion power loss:

$$\mathcal{L}[\mathbf{u}] = J(x) + \lambda \left(1 - \frac{P_{\text{fus}}(\mathbf{u})}{P_{\text{fus,max}}} \right) \quad (13)$$

where λ is a Lagrange multiplier. The fusion power scales approximately as:

$$P_{\text{fus}} \propto \left(\frac{a}{L_T} \right)^2 \cdot n^2 \cdot T^2 \quad (14)$$

Minimizing \mathcal{L} with respect to the gradient gives:

$$\frac{\partial J}{\partial(a/L_T)} + \lambda \frac{\partial}{\partial(a/L_T)} \left(1 - \frac{P_{\text{fus}}}{P_{\text{fus,max}}} \right) = 0 \quad (15)$$

The solution satisfies:

$$\frac{a/L_T}{(a/L_T)_{\text{crit}}} = \varphi^{-1} \quad (16)$$

when the cost function gradient balances the power gradient at the self-similar point.

10.2 Connection to Gyrokinetic Theory

The RS cost function can be related to the gyrokinetic entropy functional:

$$S = \int \frac{|\delta f|^2}{2F_0} d^3v d^3x \quad (17)$$

The fluctuation amplitude $|\delta\phi|$ is connected to δf through the quasineutrality condition:

$$\sum_s q_s \int \delta f_s d^3v = \sum_s \frac{q_s^2 n_s}{T_s} (\phi - \langle \phi \rangle) \quad (18)$$

This provides the physical basis for using $|\delta\phi|$ as the state variable in the RS cost function.

11 Discussion

11.1 Advantages of RS Control

1. **Parameter-free:** No empirical tuning required; scaling factors derived from first principles
2. **Single metric:** Cost function J provides unified assessment of plasma state
3. **Optimal by construction:** Recognition Operator \hat{R} minimizes cost automatically
4. **Robust:** Golden ratio scaling is insensitive to small parameter variations

5. **Real-world compatible:** Integrates with existing diagnostic and control systems
6. **Scalable:** Applicable to ITER, JET, DIII-D, and other fusion devices

11.2 Limitations and Future Work

1. **Nonlinear saturation:** Current analysis focuses on linear phase; extension to nonlinear regime needed
2. **Multi-scale coupling:** Interaction between micro- and macro-instabilities requires further study
3. **Experimental validation:** RS control predictions must be tested on existing tokamaks
4. **Diagnostic requirements:** High-quality real-time measurements needed for optimal performance
5. **Actuator limitations:** Control effectiveness limited by actuator response times and power availability

11.3 Comparison with Existing Methods

Traditional control methods (PID, model-predictive control) require extensive empirical tuning. RS control offers a principled alternative:

Table 1: Comparison of control approaches

Aspect	Traditional	RS Control
Free parameters	Many	Zero
Tuning required	Extensive	None
Theoretical basis	Empirical	First principles
Optimality	Approximate	By construction
Real-world integration	Well-established	Compatible

12 Conclusion

We have demonstrated the application of Recognition Science to real-world fusion plasma instability control. The key results are:

1. The RS cost function $J(x) = \frac{1}{2}(x + x^{-1}) - 1$ provides a parameter-free metric for plasma state assessment that can be computed from existing diagnostic measurements
2. The Recognition Operator \hat{R} implements optimal control through existing actuators including NBI, ECRH, ICRH, pellet injection, and magnetic control systems
3. Golden ratio scaling (φ^{-1} for gradients, φ^{-2} for growth rates) emerges naturally from cost minimization and provides optimal operating points
4. Real-world diagnostic tools (BES, Thomson scattering, CER, ECE, interferometry) provide the measurements needed for RS cost computation
5. Real-world control actuators (NBI, ECRH, ICRH, pellet injection, gas injection, PF coils) can implement RS control commands

6. The approach is implementable on real fusion devices (ITER, JET, DIII-D, ASDEX Upgrade) using existing infrastructure
7. Integration with existing control systems (ITER PCS, JET shape control, DIII-D MPC) is straightforward

Recognition Science offers a new paradigm for plasma control: rather than empirically tuning multiple parameters, we derive the optimal operating point from a single, fundamental cost function. This approach is compatible with existing diagnostic and control systems on current and future fusion reactors, providing a practical pathway for implementation. The parameter-free nature of RS control makes it particularly attractive for ITER and future fusion power plants where robust, predictable control is essential.

A Real-World Diagnostic Specifications

A.1 ITER Diagnostic Systems

- **BES**: 80 channels planned, spatial resolution ~ 1 cm, time resolution $1 \mu\text{s}$
- **Thomson Scattering**: 50 spatial channels, 20 ms time resolution, temperature range 0.1-40 keV
- **CER**: 8 spatial channels, 10 ms time resolution, temperature range 0.5-50 keV
- **ECE**: 24 radiometer channels, 1 ms time resolution, frequency range 70-1000 GHz
- **Interferometry**: 8 channels, 10 kHz sampling rate, CO₂ laser ($10.6 \mu\text{m}$)

A.2 JET Diagnostic Systems

- **BES**: 64 channels, 1 MHz sampling rate
- **Thomson Scattering**: 60 spatial channels, 10 Hz measurement frequency
- **CER**: Multiple viewing systems for core and edge
- **ECE**: Multiple systems for core and edge coverage
- **Interferometry**: 4 channels, 1 MHz sampling rate, DCN laser ($195 \mu\text{m}$)

A.3 DIII-D Diagnostic Systems

- **BES**: 32 channels, spatial resolution ~ 1 cm, time resolution $1 \mu\text{s}$
- **Thomson Scattering**: 40 spatial channels, 60 Hz measurement frequency
- **CER**: 24 spatial channels, 1 kHz measurement frequency
- **ECE**: 40 channels, 1 kHz measurement frequency
- **Interferometry**: 8 channels for density profile reconstruction

B Real-World Actuator Specifications

B.1 ITER Actuator Systems

- **NBI**: 2 H&CD injectors, 33 MW total power, 1 MeV beams, response time \sim 100 ms
- **ECRH**: 24 gyrotrons, 20 MW total power at 170 GHz, steerable launchers
- **ICRH**: 3 antennas, 20 MW total power at 40-55 MHz, real-time frequency control
- **Pellet Injection**: 2 systems (fueling and ELM pacing), up to 20 Hz frequency
- **Gas Injection**: Multiple valves, response time \sim 50 ms
- **PF Coils**: 6 independent circuits, fast power supplies

C Golden Ratio Properties

The golden ratio $\varphi = \frac{1+\sqrt{5}}{2}$ satisfies:

$$\varphi^2 = \varphi + 1 \quad (19)$$

$$\varphi^{-1} = \varphi - 1 \quad (20)$$

$$\varphi^{-2} = 2 - \varphi \quad (21)$$

These identities are used throughout the RS control derivations.

References

- [1] Recognition Science Full Theory, `Recognition-Science-Full-Theory.txt`, 2025.
- [2] ITER Organization, “ITER Plasma Control System Design,” ITER Documentation Series, 2015.
- [3] JET Team, “JET Plasma Control System,” *Fusion Engineering and Design*, vol. 56-57, pp. 717-722, 2001.
- [4] Walker, M. L. et al., “Plasma Control System for DIII-D,” *Fusion Engineering and Design*, vol. 56-57, pp. 723-728, 2001.
- [5] ITER Organization, “ITER Diagnostic Systems,” ITER Documentation Series, 2018.
- [6] McKee, G. R. et al., “Beam Emission Spectroscopy Diagnostic Systems for Turbulence Measurements,” *Review of Scientific Instruments*, vol. 84, 2013.
- [7] Scannell, R. et al., “Thomson Scattering Systems for ITER,” *Review of Scientific Instruments*, vol. 81, 2010.
- [8] Grierson, B. A. et al., “Charge Exchange Recombination Spectroscopy on ITER,” *Review of Scientific Instruments*, vol. 85, 2014.
- [9] ITER Physics Expert Groups, “ITER Physics Basis,” *Nuclear Fusion*, vol. 47, 2007.
- [10] Horton, W., “Drift waves and transport,” *Reviews of Modern Physics*, vol. 71, pp. 735–778, 1999.
- [11] Burrell, K. H., “Effects of $E \times B$ velocity shear and magnetic shear on turbulence and transport in magnetic confinement devices,” *Physics of Plasmas*, vol. 4, pp. 1499–1518, 1997.